Understanding the separation of anion mixtures by TiO2 membranes: Numerical investigation and effect of alkaline treatment on physicochemical properties

Patrick Dutournié, Sébastien Déon, Lionel Limousy

Version of Record: https://www.sciencedirect.com/science/article/pii/S1385894719301330
Manuscript_404225972e252fdbd7a39580d6e8042a

Understanding the separation of anion mixtures by TiO_2 membranes: numerical investigation and effect of alkaline treatment on physicochemical properties

Patrick Dutournié[1], *Sébastien Déon*[2]*, *Lionel Limousy*[1]

1- Institut de Science des Matériaux de Mulhouse (IS2M-UMR CNRS 7361), Université de Haute-Alsace, 15 Rue Jean Starcky, BP 2488, 68057 Mulhouse cedex, France

2- Institut UTINAM (UMR CNRS 6213), Université de Bourgogne-Franche-Comté, 16 route de Gray, 25030 Besançon cedex, France

Submitted to

Chemical Engineering Journal

2018

* Corresponding author

E-mail address: sebastien.deon@univ-fcomte.fr (S. Déon)

Abstract

Mechanisms governing the rejection of ions from multi-ionic solutions, and especially the selectivity between various anions are not fully understood at the present time. In this study, it is proposed, in a first part, to investigate the evolution of electric and dielectric exclusion mechanisms when anions are mixed in a solution. For this purpose, the volumetric membrane charge X_d and the dielectric constant of the solution confined within pores ε_p are numerically assessed from rejection curves with a classic transport model. This study highlights that the rejection of the various anions is differently governed by electric and dielectric mechanisms but their contribution to mixture separation seems to be proportionally impacted by the solutions mixed. It was for instance demonstrated that the couple (ε_p, X_d) obtained with the ternary salt mixture (NaF-NaI-Na_2SO_4) corresponds to the barycenter of the triangle made by the couples of the three corresponding binary salt mixtures (*i.e.* NaF-NaI, NaF-Na_2SO_4 and NaI-Na_2SO_4). In a second part, the influence of a mild alkaline treatment, consisting in the filtration of a sodium carbonate solution, is investigated from the variation in membrane charge and dielectric constant assessed from ion mixtures. It is shown that the alkaline treatment mostly diminishes dielectric exclusion through a notable increase in dielectric constant inside pores when solution contains fluoride ion. Membrane charge estimated with solutions containing fluoride ion was found to be slightly impacted, but differently depending on the other anions in solution. Finally, exclusion mechanisms are found to be weak and unaffected by the treatment when solution does not contain fluoride ion.

Keywords

Titania ultrafiltration membranes; ion rejection; alkaline treatment; physicochemical properties; transport modelling.

1. Introduction

Membrane separation processes are widely used for industrial operations due to their interesting performances in terms of flux and rejection [1]. Among these techniques, nanofiltration and low cut-off ultrafiltration processes are often implemented to separate, rectify or concentrate small solutes because they are energy efficient, user-friendly and do not require additional chemical compounds [2]. These techniques are relevant to solve many issues in various industries [3-7]. For instance, nanoporous membranes can be relevant options for the removal of pollutants from discharged effluents, such as dyes (*e.g.* rhodamine-B and congo red), heavy metals (*e.g.* Pb^{2+}, Cu^{2+}, Cd^{2+}, Cr^{3+}) or medicinal residues (*e.g.* antibiotics or hormones) from textile, chemical and pharmaceutical industries, respectively [8, 9]. They are also competitive for the concentration of target species such aroma from juice, serum proteins from milk in food industry [10], or fractionation/purification of natural or synthesized active substances with high added-value (*e.g.* phenolic compounds, antioxidants, anthocyanins) in biotechnological and pharmaceutical industries [11, 12]. Membranes used in pressure-driven processes can be either organic (polymer) or mineral (ceramic) [13]. The latter enable working in hard conditions such as mechanical stress, pH, organic solvents, temperature, etc. [14]. Moreover, they are much less prone to biofilm development and can thus be more easily cleaned [15, 16]. However, they are generally more expensive and less efficient (ratio of filtration performances and process compactness) than organic membranes. Consequently, they are not widely implemented for industrial purposes, and their use is limited to specific applications which do not allow the use of organic materials. The most commonly used membranes are constituted of an active layer in metal oxide as titania, alumina or zirconia. In the field of pressure-driven filtration, these membranes are usually preferred above organic membranes when their additional physicochemical properties are required (petrochemistry, metallurgy, pigments, pharmaceuticals, solar cells, etc.) [17]. For instance, titania membranes induce interesting interactions with ions in solution, coupled with antifouling, antibacterial and

photo-catalytic properties [18-21]. Mozia et al. [22], who studied the antifouling properties of a TiO_2 membrane, attribute these properties to the amphoteric and hydrophilic character of the surface. Choi et al. [23] have synthesized TiO_2 membranes with hierarchical multilayer structure for photo-catalytic purpose. Hou et al. [24] have also prepared membranes coated with titania nanoparticles for CO_2 conversion. They observed a decrease of contact angle after coating and an increase of the membrane efficiency. As a general statement, surface properties of the membrane depend on the pH of the solution and the ionic species in the solution (nature and concentration). Indeed, the interactions between ions and surface (attractive or repulsive forces, ion adsorption, etc.) are responsible for the modification of overall membrane properties, especially the membrane surface charge [25, 26]. In this context, the study of ceramic membrane performances is therefore of prime importance [27, 28]. Most of research studies were focused on the investigation of single salt filtration [29, 30] or common salt mixtures solutions [28] in specific operating conditions (concentration, pH, temperature, etc.). In their works, authors usually analyzed results only by considering steric hindrance and electrostatic interactions between the surface and the ionic solutes in solution. Few authors cared about interactions from other causes. Indeed, it was shown that dielectric effects, which are the sum of different contributions (confinement, modification of electric field line, interactions dipole / solvent, dipole / ion, charge / solvent, ion polarizability, etc.), should be considered to discuss the performances of nanofiltration process due to their small pore size [31-34]. Two mechanisms are usually considered in literature to describe the increase in the interaction energy due to dielectric exclusion, namely Born and “image charges” effects. In literature, solvation energy barrier described Born model is usually considered solely [31] but some authors have considered that only the effect of “image charges” are sufficient to describe dielectric exclusion (*i.e*. dielectric properties of the solution inside pores are equal to those of the feed solution) [35], when others consider that both contribute to exclusion [36]. In this study, it is considered that all the dielectric exclusion mechanisms are governed by a decrease

in the apparent dielectric constant of the solution within the membrane pores. However, dielectric constant of solution confined in pores is difficult to estimate experimentally since no direct measurement inside nanopores can be implemented. It is only possible to estimate an overall dielectric constant of the soaked membrane by electrochemical impedance spectroscopy and estimate the contribution of the confined solution through porosity [37]. Unfortunately, with NF membranes, porosity of the skin layer is very low and uncertainties are therefore very large. Moreover, the contribution of the support layer on the overall measurements is tremendous and that of the skin layer usually lost and undetectable. Hence, this technique requires to isolate the thin skin layer (thickness close to 100 nm), which is not necessarily easy [38, 39]. For this reason, a numerical assessment by fitting filtration performances is often preferred [40]. Although these phenomena are usually neglected with ultrafiltration membranes, such as titania membranes, a previous study has shown that they have a major impact on rejection [41]. Indeed, it was observed that the rejection rates of single salt solutions are significantly influenced by a mild alkaline treatment, while surface charge and steric hindrance remain almost unchanged. The main conclusion was thus that the surface chemistry of the active layer, and thus the interactions between surface and ions impacted the dielectric exclusion of halide ions. Although interesting trends were highlighted, firm conclusions could not be drawn from single salt solutions since electric and dielectric contributions could not be decoupled.

The main objective of the present work is to investigate the selectivity performances of a titania UF membrane in the case of ionic mixtures. For this purpose, separation performances of ionic mixtures were numerically interpreted by considering both electric and dielectric effects. Additionally, the influence of a specific mild alkaline treatment (sodium carbonate) on surface properties and filtration performances is more specifically investigated.

2. Material and methods

Filtration experiments were performed with a laboratory pilot plant in stainless steel [42], provided by TIA (Techniques Industrielles Appliquées, Bollène, France), which is equipped with a commercial tubular TiO_2 membrane (7 mm inner diameter vs. 25 cm length) provided by TAMI Industries (Nyons, France). The feed aqueous solution is contained in a tank (5 L), and the flow-rate and pressure in the system are provided by a volumetric pump. Filtrations were performed at a temperature of 25°C (controlled by a cooling unit) and for a flow rate of 700 L/h, corresponding to a Reynolds number higher than 35,000. The flow is mainly turbulent avoiding concentration polarization at the surface vicinity. The pressure is adjusted via a manual valve and is continuously measured by two analogic sensors located before and after the membrane. Feed and retentate solutions are recycled in the feed tank during filtration (except for sampling) to keep feed concentrations constant and avoid performance variations over time [43]. For each pressure, permeation stream is sampled for weighting and analysis. Before experiments, the membrane is conditioned by filtrating pure water up to reach steady hydraulic performances. Permeation of pure water is also performed (demineralized water, conductivity < 0.1 µS/cm) to estimate the membrane hydraulic permeability.

In a second step, Vitamin B12 (Alfa Aesar, purity 98%) was filtered to estimate the mean pore radius of the membrane in the various conditions. The sample concentrations were measured by absorbance measurements at 362 nm with an UV-visible spectrophotometer (Lambda 35, Perkin Elmer Instrument, Waltham, MA, USA). Filtration of saline aqueous solutions were implemented with four salts (alone or in mixture), namely NaF, NaCl, NaI and Na_2SO_4 (Sigma-Aldrich, St. Quentin Fallavier, France, purity > 99%), with the same sodium concentration ($[Na^+]$ = 5 mol m^{-3}). The various monovalent halide ions were chosen for their differences in ionic radius, ionization energy, electronegativity, whereas SO_4^{2-} was chosen as a reference polyatomic divalent anion. Permeate (C_p) and retentate (C_r) samples were

analyzed by conductimetry (conductimeter GLP 31, Crison, Estella, Spain) for single salt solutions and by ionic chromatography (883 Basic IC Plus, Metrohm, Courtaboeuf, France) for salt mixtures.

The observed rejection rate R_i is calculated by using Eq. 1 and plotted as a function of the permeation flux (J_v) calculated by sample weighting.

$$R_i = \frac{C_{i,r} - C_{i,p}}{C_{i,r}} \quad (1)$$

Before each test, the hydraulic permeability was estimated from pure water filtration by measuring the permeation flux of pure water (J_w) for various applied pressures (ΔP). The membrane hydraulic permeability (L_p) is calculated from the slope of the linear curve by using Eq. 2, knowing the solution viscosity μ:

$$J_w = \frac{L_p}{\mu} \Delta P \quad (2)$$

The membrane was treated by the filtration of an alkaline solution (sodium carbonate solution, 6.6 mol m^{-3}, pH ≈ 10.5) during 2 hours to modify its surface properties. After rinsing, the experiments were repeated following the same procedure.

Pore size was also estimated by scanning electron microscopy (Philips XL30 FEG, SEMTech Solutions, North Billerica, MA, USA). Evolution with pH of membrane charge in contact with various solutions (water alone or with salts at 5 mol m^{-3}) was assessed by zetametry experiments (Nano ZS, Malvern Instrument, Orsay, France) to discuss about electrostatic interactions.

3. Numerical modelling

Several works were devoted to the numerical study of mass transfer through ultra- or nanofiltration membranes. Three main approaches are commonly used in literature to describe transport within pores. The Maxwell-Stefan approach [44] describes the flux of each specie as the sum of the effect of generalized driving forces. This requires the knowledge of different parameters that are very difficult to estimate, leading to a low uptake. The second approach derives from the thermodynamic theory of irreversible processes [45]. It is often used owing to its simple numerical implementation, but the significant number of assumptions causes the loss of physical description. The last approach, based on Nernst-Planck equation, comes from the thermodynamics of irreversible processes by simplifying some terms in the equation and by taking physical behavior into account with a complementary description [46-48]. In the common case, the transport is assumed to be mono-dimensional within uniform and cylindrical pores. The ionic solute transport is described by the sum of three contributions (convection, diffusion and electro-migration) [36]. The flux of each solute is described in steady state by Eq. 3:

$$j_i(x) = -c_i K_{i,d} D_{i,\infty} \frac{d\left[\ln \gamma_{i,p}\right]}{dx} - K_{i,d} D_{i,\infty} \frac{dc_i}{dx} - \frac{z_i c_i K_{i,d} D_{i,\infty}}{RT} F \frac{d\psi}{dx} + K_{i,c} c_i V = V C_{i,p} \quad (3)$$

The distribution of ion concentrations at both sides of the active layer is described by an equilibrium partitioning at the interfaces between bulk and pore solutions [49, 50]. This equilibrium consists in an equality of generalized chemical potentials of each solute at the interface. Physically, the ratio between the concentration inside pores c_i and that of the retentate or permeate streams C_i ($C_{i,r}$ or $C_{i,p}$ depending of the interface considered) is commonly described by the product of three contributions, namely steric, electric and dielectric.

$$\frac{c_i}{C_i} = \frac{\gamma_{i,s}}{\gamma_{i,p}} \phi_i \exp(-\Delta W_i) \exp(-\frac{z_i}{RT} F \Delta\psi_D) \quad (4)$$

where $\phi_i = \left(1 - \frac{r_{i,s}}{r_p}\right)^2$ is the steric partitioning coefficient depending on the ratio of pore and solute radii[51]. $\Delta\psi_D$ is the difference in electrical potential at both sides of the interface free solution/solution in the pore, also called Donnan potential.

ΔW_i represents the dielectric effects, which are a sum of different interactions between ions and membrane, such as the difference of solvent dielectric constant, the influence of the surface chemistry, etc. This contribution is considered in the model by attributing the modification of dielectric exclusion to a variation of the apparent dielectric permeability of the pore solution ε_p in the Born model (Eq. 5) [52].

$$\Delta W_{i,born} = \frac{(z_i e)^2}{8\pi\varepsilon_0 r_{i,s} k_B T}\left(\frac{1}{\varepsilon_p} - \frac{1}{\varepsilon_b}\right) \quad (5)$$

All the previous equations are given for the ith ion, and sets of all the ions are linked by electroneutrality condition in bulk (Eq. 6) and pore (Eq. 7) solutions.

$$\sum_{i=1}^{n} z_i C_i = 0 \quad (6)$$

$$\sum_{i=1}^{n} z_i c_i + X_d = 0 \quad (7)$$

where X_d represents the volumetric membrane charge density.

The permeation flux is calculated from Eq. 8 by taking the effect of the osmotic pressure $\Delta\pi$ into account.

$$J_v = \frac{L_p}{\mu}(\Delta P - \Delta\pi) \quad (8)$$

This model requires 4 physical parameters (L_p, r_p, ε_p and X_d) but only ε_p and X_d are studied in this study since the others are experimentally assessed.

For one couple (ε_p, X_d), the boundary conditions (ion concentrations) at the pore entry are firstly calculated by coupling Eq. 4 with bulk and pore electroneutrality conditions (Eq. 6 and 7). Then concentration gradients along the pore length are estimated by solving the differential Eq. 3 for each ion. Finally, permeate concentrations are calculated from concentrations at the pore outlet with Eq. 4 and electro-neutrality conditions. The numerical scheme is explicit and iterative until convergence of the various permeate concentrations is reached. The rejection rates are directly calculated from ion concentration in the permeate compartment and plotted versus the permeation flux calculated with Eq. 8. In this study, ε_p and X_d are numerically and simultaneously adjusted by fitting experimental results with the model. This fitting procedure is processed by Levenberg–Marquardt algorithm, which solves nonlinear problems with Gauss–Newton algorithm and the method of gradient descent [52].

The average pore radius is estimated by numerically approximating the rejection rate of a neutral solute (Vitamin B12) with the same equations, for which electric and dielectric contributions are neglected in equations 3 and 4. The set of equations can be analytically solved and leads to Eq. 9 [53].

$$R_i = 1 - \frac{\phi_i K_{i,c}}{1 - \left(1 - \phi_i K_{i,c}\right) \exp\left(- \frac{K_{i,c} r_p{}^2 \Delta P}{8 \mu K_{i,d} D_\infty} \right)} \tag{9}$$

4. Results and Discussion

A previous work has shown interesting trends concerning the evolution of ion rejection and parameters with single salt solutions after a mild alkaline treatment [41]. The alkaline treatment was found to significantly increase rejection rates of NaCl and NaBr, whereas NaF rejection rate was decreased. Oppositely, the rejection of NaI and Na_2SO_4 were almost unchanged. The main mechanism implied in this rejection modification after treatment was probably a significant modification of dielectric exclusion. However, conclusions drawn in this previous study were questionable since numerical results were discussed only from single salt solutions. In this case, exclusion mechanisms have the same influence on rejection and an in-depth study from ion mixtures is required to draw accurate conclusions. The first aim of this study thus lies in the understanding of anion rejection mechanisms from the filtration of ion mixtures before discussing the impact of a mild alkaline treatment on separation selectivity, and especially the impact on electric and dielectric exclusion mechanisms.

4.1. Understanding of anion rejection mechanisms

First of all, the permeation of pure water and the rejection of Vitamin B12 were investigated for structural characterization. Hydraulic permeability L_p was estimated from the slope of the evolution of water flux with applied pressure and a value of 5.5 10^{-14} m^3 m^{-2} was obtained. The mean pore radius r_p was also identified by adjusting its value in Eq. 9 to fit the evolution of VB12 rejection rate with permeation flux (*cf.* Fig. 1), as it is usually done in literature for nanoporous membranes [54, 55]. A mean pore radius of 2.3 nm was found, which means that steric exclusion mechanism at the pore entry has probably a very little influence on ion rejection.

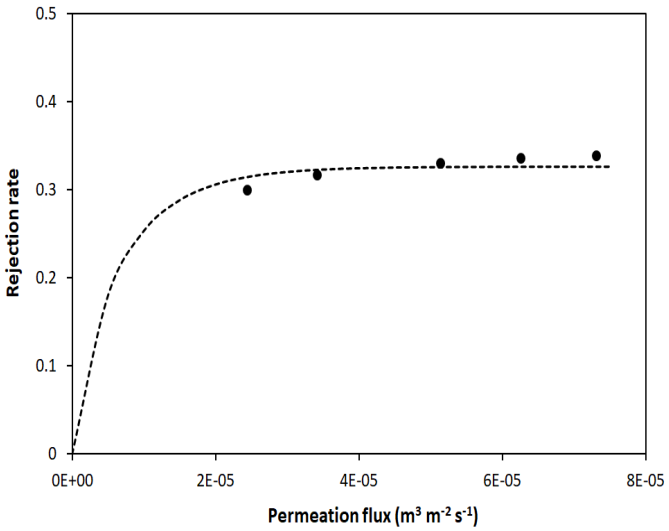

Figure 1. Experimental (symbols) and numerical (lines) evolutions of Vitamin B12 rejection rate with permeation flux.

Scanning electron microscopy image of the membrane surface is also provided in Fig. 2 to discuss about this mean pore size estimated indirectly from VB12 rejection. From this figure, it appears that surface porosity is induced by either large crack-like pores (4-9 nm) or smaller intergranular pores (close to nanometer) which are less discernible by SEM. This distribution is consistent with our mean hydrodynamic pore diameter estimated from rejection of VB12 by considering cylindrical pores (~4.6 nm).

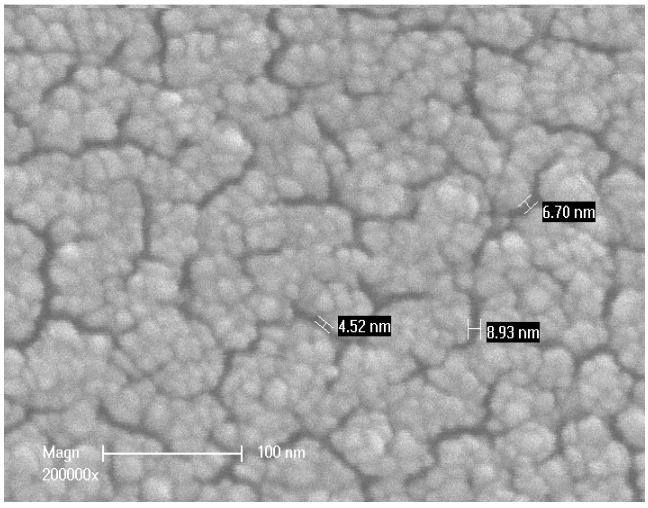

Figure 2. SEM image of the membrane surface.

To investigate the other mechanisms involved in anions rejection by TiO_2 membranes, various ionic solutions containing salts (alone or in mixture) were filtered and the values of maximum rejection rates obtained for each solution are summarized in Table 1.

First, it can be observed that sulfate ion is almost not retained in the absence of fluoride ions (*i.e*. 4% alone and 2 % with iodide ions). Conversely, the rejection rate of sulfate increases significantly in the presence of fluoride ions, reaching 53 and 63%, in ternary and quaternary mixtures, respectively. The same behavior is observed with iodide and chloride ions, but to a letter extent. As previously observed, the fluoride ions modify the interactions between the surface and the ionic species, but it is always mainly rejected compared with the others monovalent ions. For instance, Fig. 3 shows the rejection curves of NaCl and NaF ($[Na^+]$ = 5 mol m^{-3}) when these salts are alone in solution (Fig. 3a) and when they are mixed (Fig. 3b).

Table 1. Experimental rejection rates for single salt solutions and salt mixtures.

	Maximum rejection rate (%)			
Solutions	F^-	Cl^-	I^-	$SO4^{2-}$
NaF	**42**	-	-	-
NaCl	-	**15**	-	-
NaI	-	-	**3**	-
Na_2SO_4	-	-	-	**4**
NaF-NaCl	**30**	**22**	-	-
NaF-NaI	**36**	-	**27**	-
NaF-Na_2SO_4	**23**	-	-	**63**
NaI-Na_2SO_4	-	-	**0**	**2**
NaF-NaI-Na_2SO_4	**16**	-	**8**	**53**

From Fig. 3, it can be seen that the rejection curves of ions obtained with the salt mixture are intermediary between those of single salt solutions (*i.e*. the rejection rate of fluoride ion decreases in mixture when that of chloride ion increases).

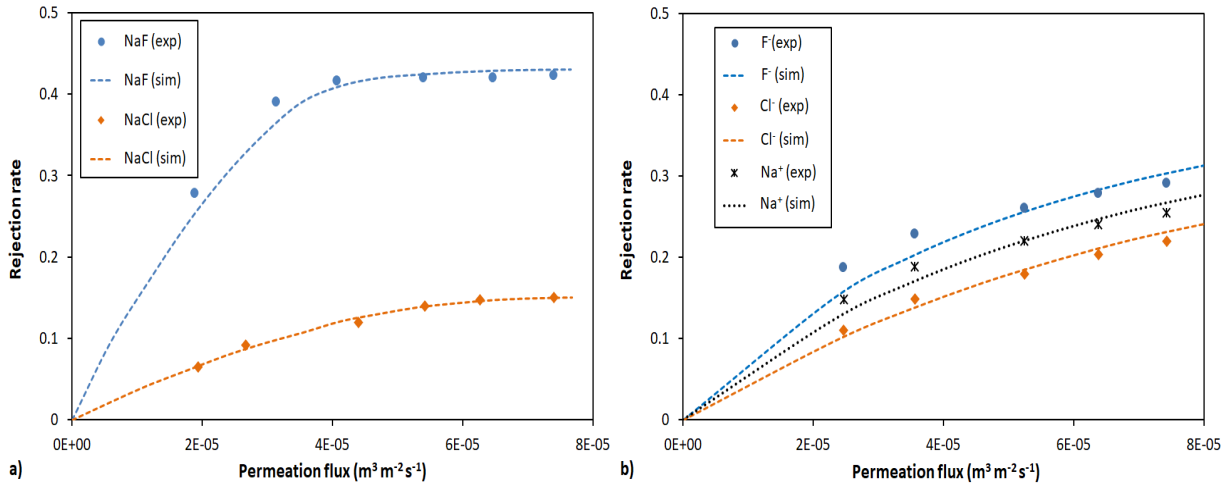

Figure 3. Experimental (symbols) and numerical (lines) evolutions of ion rejection rate with permeation flux for NaF and NaCl alone (a) and in mixture (b).

This behavior in the presence of fluoride ion is unexpected since this ion exhibits similar properties than other halide ions such as chloride or iodide. In order to understand why the presence of fluoride has a considerable impact on anion rejection, the membrane zeta-potential was investigated with water, NaCl and NaF solutions, and the evolutions with pH are provided in Fig. 4.

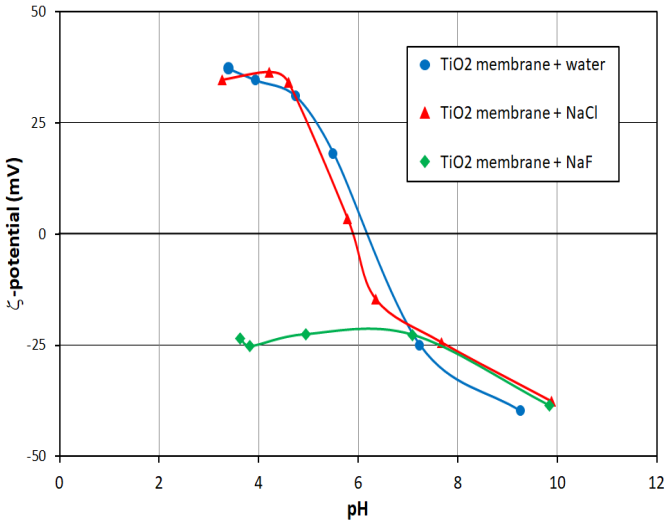

Figure 4. Evolution of z-potential with pH measured with water, NaCl and NaF solutions.

From Fig. 4, it can be seen that the presence of chloride has a very weak influence on membrane charge, irrespective of the pH considered. The membrane is positive at low pH-values and becomes negative in basic conditions due to the amphoteric behavior of titania. The isoelectric point of the membrane is close to 6 when solution does not contain fluoride ions, which is consistent with values reported in literature [56]. However, with NaF, the membrane charge was found to be strongly negative irrespective of the solution pH, probably due to a strong adsorption of fluoride ion. Indeed, ζ-potential is constant (almost -25 mV) for pH up to 7, which means that the membrane charge induced by amphoteric groups of TiO_2 is completely screened by adsorption. For pH higher than 7, the overall negative charge increases due to the non-negligible impact of the negative charge induced by amphoteric titania.

At the pH of the filtration experiments (6-6.2), membrane is almost neutral when solution does not contain fluoride ion since this value is close to membrane pie. Hence, anions are weakly rejected. Oppositely, in the presence of fluoride, overall membrane charge is strongly negative due to fluoride adsorption, which necessarily leads to high rejection of anions, and especially that of divalent ions such as sulfate.

All these trends, which can be observed on rejection curves (Fig. 3), can also be investigated through the evolution of the dielectric constant of solution inside pores ε_p and the membrane charge density X_d. For this purpose, the rejection curves were fitted with the transport model by adjusting these two parameters, as it is illustrated in Fig. 3a and 3b.

For example, the best-fitted parameters estimated from the rejection curves of single NaCl and NaF solutions and their mixture (lines in Fig. 3) are provided in Fig. 5.

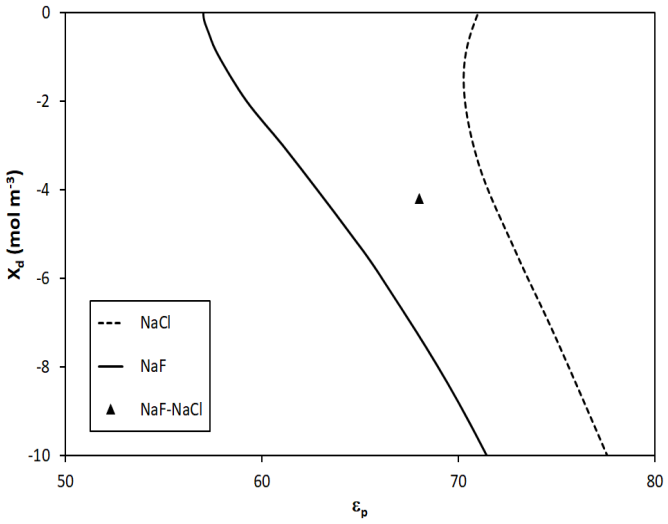

Figure 5. Best-fitted couples (ε_p, X_d) assessed by numerical approximation of the experimental ion rejection curves obtained with solutions of single NaCl, single NaF and NaCl-NaF mixture ([Na^+] = 5 mol m^{-3}).

As observed in Fig. 5, it exists an infinite number of couples (ε_p, X_d), which can well describe the rejection curves of a single salt (lines in Fig. 5). Indeed, a decrease of the dielectric constant (*i.e*. an enhancement of dielectric exclusion) can be balanced by a decrease of the membrane charge (*i.e*. a decline of electrostatic interactions) since both phenomena have the same impact on a salt rejection curve. For this reason, it is difficult to conclude about the influence of a treatment from those parameters when they are assessed from single salts. Oppositely, with salt mixtures (solutions containing three or more ions), the number of adjustable parameters is lower than the number of ion rejection curves. In this case, dielectric exclusion (ε_p) and electrostatic interactions (X_d) have a different influence on ion rejection and only one couple (ε_p, X_d) can describe the various rejection curves simultaneously. Indeed, an increase in dielectric exclusion leads to an enhancement of rejection (irrespective of the ion considered), whereas an increase in electrostatic interactions leads to an enhancement of the separation selectivity between ions [32]. In the case of NaCl-NaF mixture (Fig. 3b), the couple (ε_p = 68, X_d = -4 mol m^{-3}, corresponding to the symbol in Fig. 4) correctly describe the three rejection curves provided in Fig. 3b.

Only negative values of X_d are considered in Fig. 5 since zetametry investigation (Fig. 4) has shown that the pH of solutions is always equal or higher than the membrane isoelectric point and the membrane charge is therefore always negative (or neutral), irrespective of the solution filtered.

The major conclusion that can be drawn from Fig. 5 is that the point corresponding to the couple of best-fitted parameters (ε_p, X_d) for the salt mixture NaF-NaCl is midway between the curves representing the infinite number of couples for the two single salts NaF and NaCl.

For a further discussion, the same analysis was implemented for other mixtures containing two or three salts, namely NaI-Na_2SO_4, NaF-Na_2SO_4, NaI-NaF and NaI-NaF-Na_2SO_4. The various ion rejection curves (experimental and simulated) obtained for each of these mixtures are drawn in Fig. 6. The corresponding best-fitted couples (ε_p, X_d) are provided in Fig. 7 for comparison with curves assessed from single salts.

For all the studied solutions, the simulated curves closely approximate the experimental rejection rates, while only a couple of parameters is adjusted for approximating the three or four curves (Fig. 6). It should be noted that rejection curves obtained with the mixture NaI-Na_2SO_4 are not provided here since rejection rates were lower than 5%. However, a best-fitted couple has been successfully assessed from these curves.

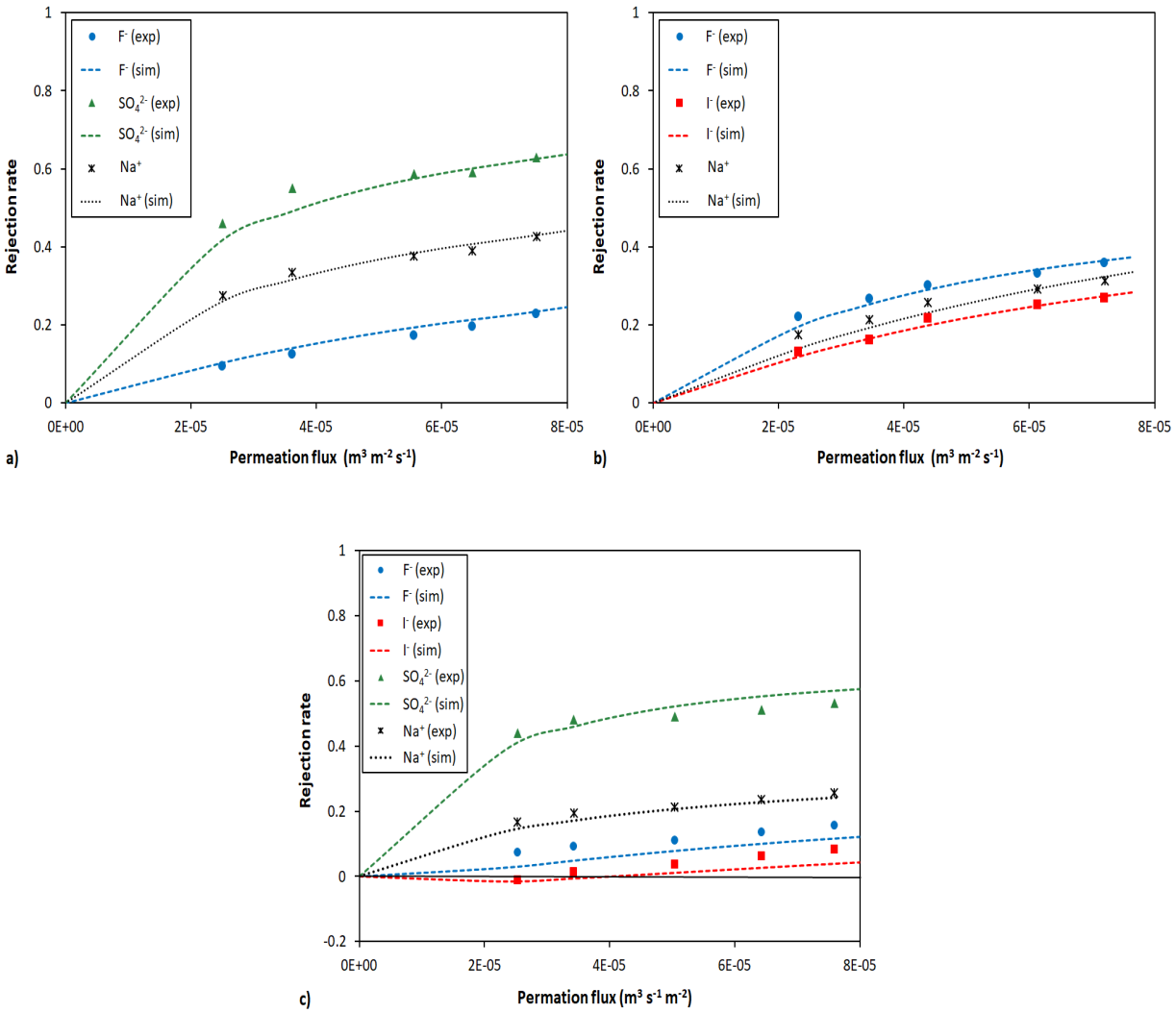

Figure 6. Experimental (symbols) and numerical (lines) evolutions of ion rejection rate with permeation flux for the various salt mixtures investigated:
a) NaF-Na_2SO_4, b) NaF-NaI and c) NaF-NaI-Na_2SO_4 mixtures

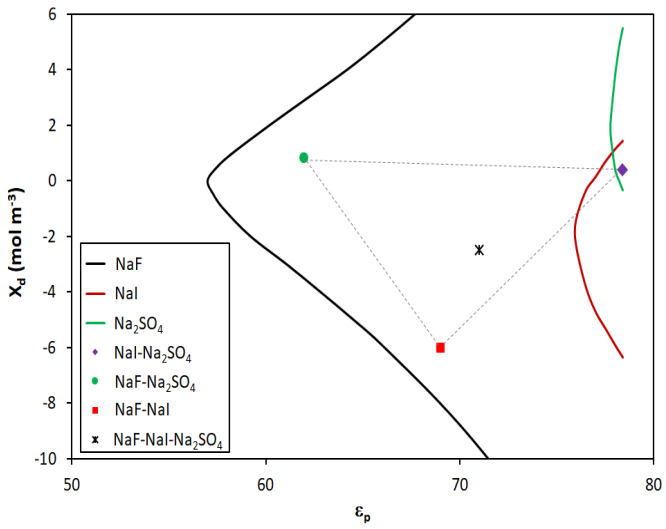

Figure 7. Best-fitted couples (ε_p, X_d) assessed by numerical approximation of the experimental ion rejection curves for single salts (lines) and mixtures provided in Fig. 4 (symbols).

From Fig. 7, it appears that the points representing the couple of best-fitted parameters obtained for mixtures of two salts are located between curves (representing the infinite number of couples (ε_p, X_d)) obtained for the two single salts, irrespective of the salts considered. For instance, the best couple (ε_p, X_d) assessed with NaI-Na_2SO_4 mixture show almost the same dielectric constant than single salts and a surface charge in the overlapping region between curves of single salts. This means that, when sulfate ions replace iodide, the membrane charge is reversed and becomes slightly positive. If these two ions are mixed, the membrane charge becomes close to zero. It can also be seen that the membrane charge seems to be slightly positive for mixtures containing sulfate ions for the two binary salt mixtures (NaI-Na_2SO_4 and NaF-Na_2SO_4), whereas it remains negative when solution contains only iodide and fluoride ions (NaI-NaF). Hence, it can be concluded that sulfate ion has mainly a strong impact on membrane charge X_d. Oppositely, the dielectric constant ε_p was found to strongly decrease due to the presence of fluoride ions, either alone or in mixture (with NaI or Na_2SO_4). This trend is also observable on rejection curves (Fig. 6) since the rejection of sulfate is significantly enhanced in the presence of fluoride, *i.e.* rejection rate of sulfate

increases from 4% alone to more than 50% with fluoride. Concerning the rejection of fluoride, it depends of the other ions present in the solution ($R_{F^-}(SO_4^{2-}) < R_{F^-}(Cl^-) < R_{F^-}(I^-) < R_{F^-}(\text{alone})$).

Similar trends are obtained for the ternary salt mixture (containing NaI-NaF-Na_2SO_4) for which surface charge is increased due to sulfate presence (*i.e.* compared with NaF-NaI mixture) and the dielectric constant is decreased due to the presence of fluoride (*i.e.* compared with NaI-Na_2SO_4 mixture).

Finally, the main conclusion that can be drawn from Fig. 7 is the fact that the couple (ε_p, X_d) obtained for the mixture of the three salts (ε_p = 71.0, X_d = -2.5 mol m^{-3}) corresponds the barycenter of the triangle composed by the couples obtained with the binary salt mixtures (ε_p = 69.9, X_d = -1.8 mol m^{-3}). This point is relevant since it shows that ions seem to act differently on exclusion mechanisms, but when they are mixed, each ion proportionally impacts all the phenomena.

4.2. Modification of selectivity performances after alkaline treatment

It was recently shown that chemical treatments, which are often used to clean membranes, can have a strong impact on filtration performances and separation selectivity. To understand how the filtration of a mild alkaline solution can strongly modify ion rejection, a thorough numerical investigation was implemented on ionic mixtures. The same filtration experiments provided in the previous section were repeated after the filtration of a sodium carbonate solution (6.6 mol m^{-3}, pH = 10.5 approximately). The rejection rates obtained after this mild treatment are summarized in Table 2 for comparison with those obtained before treatment, experiments being carried out in the same chronologic order. It should be noted that the rejection rate of vitamin B12 and corresponding mean pore radius remain almost identical and

the hydraulic permeability variation was lower than 5% after alkaline treatment. This allows us to consider that variations of ion rejection induced by treatment cannot be attributed to structural modification and only electric and dielectric exclusions can be incriminated.

Table 2. Experimental rejection rates for mixed salt-water solutions and single salt-water solution after the alkaline treatment.

	Maximum rejection rate (%) after (before) alkaline treatment			
Solution	F^-	Cl^-	I^-	$SO4^{2-}$
NaF	**26** (42)	-	-	-
NaCl	-	**36** (15)	-	-
NaI	-	-	**8** (3)	-
Na_2SO_4	-	-	-	**2** (4)
NaF-NaCl	**17** (30)	**11** (22)	-	-
NaF-NaI	**21** 36)	-	**13** (27)	-
NaF-Na_2SO_4	**10** (23)	-	-	**48** (63)
NaI-Na_2SO_4	-	-	**3** (0)	**4** (2)
NaF-NaI-Na_2SO_4	**9** (16)	-	**0** (8)	**47** (53)

Comparison between maximum rejection rates before and after treatment shows that its impact is low for sulfate ions. Indeed, the rejection of sulfate ion is close to zero in the absence of fluoride ion (2% for sodium sulfate alone and 4 % with iodide ions). When fluoride ions are present in the solution, sulfate rejection significantly rises but in a lesser extent (48 and 47 % instead of 63 and 53 for NaF-Na_2SO_4 and NaF-NaI-Na_2SO_4, respectively). The mild alkaline treatment tends to noticeably decrease fluoride rejection, which is almost twice as low as before treatment (26 instead of 42 %). However, the decrease of rejection rate observed when mixing fluoride ions with other anions (from 26 % to 17, 21 and 10 % with Cl^-, I^- and SO_4^{2-}, respectively) remains almost the same, even though fluoride ion rejection rates are clearly lower than those before treatment. Rejection rates of chloride ions from single NaCl solution after treatment is considerably higher than that before treatment (36 instead of 15 %). Moreover, trends obtained for mixtures containing chloride ions are notably different. Indeed, its rejection is sharply decreased when mixed with fluoride ions (from 36 to 11 %), whereas it was slightly increased (from 15 to 22 %) with the same

solutions before treatment. Finally, the impact of alkaline treatment on iodide ions is difficult to discuss since rejection rates are very low. However, it can be seen that the increase in rejection induced by the presence of fluoride ions is significantly less pronounced after treatment (from 8 to 13 % instead of 3 to 27 %).

These results clearly prove that the alkaline treatment affects the physicochemical properties of the membrane surface and therefore the interactions with water and ions. Previous investigations have shown that the surface electric charge as well as the pore size remain almost the same after treatment [41]. This tends to confirm that the alkaline treatment mainly leads to a modification of the surface interactions energies between the material and the solvent (water), which is reflected by a decrease in the dielectric interactions with the surface within the pores.

This assumption is investigated by fitting rejection curves with the best couple (ε_p, X_d) and results obtained with single salt solutions (NaF, NaI, Na_2SO_4) are provided in Fig. 8.

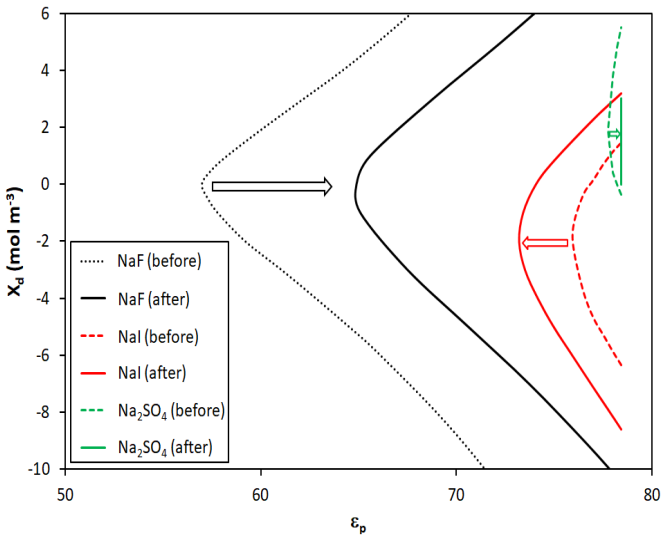

Figure 8. Best-fitted couples (ε_p, X_d) assessed by numerical approximation of the experimental rejection curves of single salts before (dotted lines) and after (solid lines) alkaline treatment.

The evolution of curves representing the infinite number of couples (ε_p, X_d) for each salt before and after the alkaline treatment seems to show that the latter mainly impacts the dielectric constant inside pores, which corresponds to a translation the whole curve along the x-axis. The translation in the direction of high ε_p value corresponds to a decrease of dielectric exclusion (*e.g.* NaF), whereas a translation in the direction of low ε_p corresponds to an increase of dielectric exclusion (*e.g.* NaI). An ε_p-value of 78.4 means that dielectric exclusion is negligible (*e.g.* Na_2SO_4). Although these trends seem pertinent, the fact that the values of ε_p and X_d are not known does not allow drawing a firm conclusion since it is possible that X_d-value also varies due to slight changes in surface properties. For this reason, couples assessed by fitting rejection curves of ion mixtures after treatment (as illustrated in Fig. 9 for the mixture containing NaF-NaI-Na_2SO_4) are also discussed further.

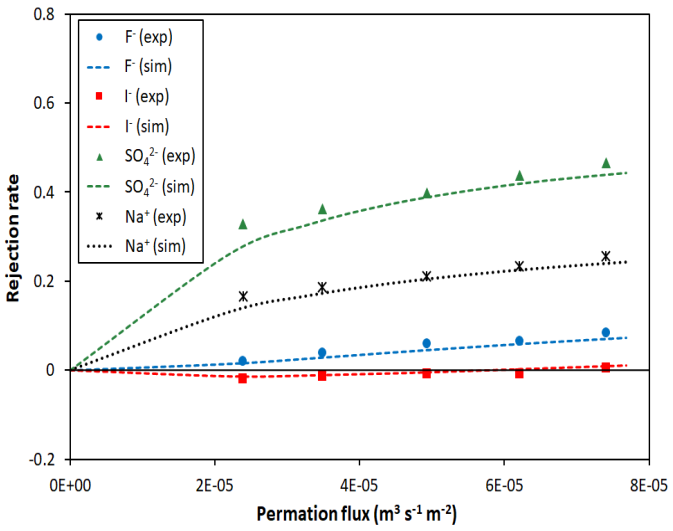

Figure 9. Experimental (symbols) and numerical (lines) evolutions of ion rejection rate with permeation flux for NaF-NaI-Na2SO4 mixture after alkaline treatment.

Rejection curves obtained with this mixture are similar to those obtained before treatment and only a slight decrease in rejection of all ions is discernible. The couples (ε_p, X_d) of all the mixtures assessed by numerical approximation of experimental rejection curves before and

after treatment are depicted in Fig. 10 to discuss the impact of the alkaline treatment in a relevant manner.

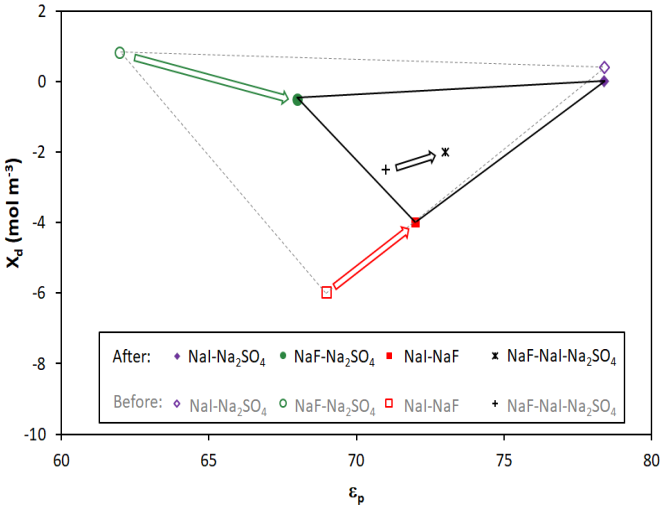

Figure 10. Best-fitted couples (ε_p, X_d) assessed by numerical approximation of the experimental ion rejection curves before and after the alkaline treatment.

From Fig. 10, it appears that the influence of each ion on the couples (ε_p, X_d) when mixing them is similar to that observed before treatment. Nevertheless, it can be concluded that the rejection mechanisms (electric and dielectric) are affected by the alkaline treatment for all the mixtures, except the NaI-Na_2SO_4 mixture, for which the values of ε_p and X_d remain almost the same. Although it was expected from single salt mixtures that only dielectric constant inside pores is affected by the treatment, the study of ion mixtures clearly demonstrates that membrane charge is also impacted. Fig. 10 indicates that the dielectric constant inside pores assessed for NaF-Na_2SO_4 and NaF-NaI mixtures is notably increased due to the alkaline treatment (translation along x-axis). Additionally, the absolute value of membrane charge was found to significantly decrease for the NaF-NaI mixture. In the case of the NaF-Na_2SO_4 mixture, the membrane charge remains very low but the sign is reversed from positive to negative.

Finally, it is also highlighted in Fig. 10 that the couple (ε_p, X_d) obtained for the ternary salt mixture (NaF-NaI-Na_2SO_4) still corresponds to the barycenter of the triangle made by the couples obtained with the three binary salt mixtures. With this mixture, the alkaline treatment thus tends to increase the dielectric constant inside pores (decrease of dielectric exclusion) and slightly decrease the negative membrane charge.

It should be mentioned that the variations obtained for membrane charge are very low, which can explain why these changes are not necessarily observable from characterization of the surface properties. Moreover, the membrane charge X_d considered in the modeling corresponds to the charge inside the membrane pores whereas the methods of characterization enable only an estimation of the membrane surface properties. These trends confirm that a numerical investigation carried out on multi-ionic mixtures is a key step to discuss about the influence of a chemical membrane modification, such as a chemical treatment, surface functionalization or membrane fouling.

5. Conclusion

In this work, the influence of the various ions present in ionic solutions on electric and dielectric exclusion was investigated through the numerical assessment of the membrane charge density and the dielectric constant of the solution inside pores. It was firstly shown that the various mechanisms governing filtration performances cannot be discussed from parameters estimated with single salt solutions. Indeed, it exists an infinity of couples (ε_p, X_d) which can describe one salt rejection curve, contrary to mixtures for which only one couple fits the various curves simultaneously. Consequently, the study of multi-ionic separation has shown that ions have a different influence on both electric and dielectric exclusion. It was also highlighted that the parameters governing electric and dielectric exclusion of ions for a complex salt mixture is a proportional combination of the values assessed from salts (or simpler salt mixtures) which were mixed. This was especially emphasized for the couple (ε_p, X_d) of a ternary salt mixture (NaF-NaI-Na_2SO_4) that corresponds to the barycenter of the triangle derived from the couples of the three corresponding binary salt mixtures (NaF-NaI, NaI-Na_2SO_4 and NaF-Na_2SO_4). Finally, this numerical study of mechanisms governing multi-ionic separation was also extended to the discussion about the impact of a chemical treatment by a mild alkaline solution. This revealed that such a treatment notably impacts dielectric exclusion through a significant increase of the dielectric constant of the solution inside pores (decline of exclusion) for solutions containing fluoride ions. Similarly, membrane charge (with solutions containing fluoride ions) was found to be slightly affected by the treatment, contrary to what was expected from characterization and filtration of single salts. Oppositely, the filtration of the solution which does not contain fluoride ion (NaI-Na_2SO_4) shows that ion rejection seems to be unaffected by the treatment, which is probably due to weak dielectric exclusion ($\varepsilon_p \sim 78.4$) and electrostatic interactions ($X_d \sim 0$).

Glossary

c_i	Concentration of ion i within the pore (mol m^{-3})
$C_{i,p}$	Permeate concentration of ion i (mol m^{-3})
$C_{i,r}$	Bulk concentration of ion i (mol m^{-3})
$D_{i,\infty}$	Diffusion coefficient of ion i at infinite dilution (m^2 s^{-1})
e	Electronic charge (1.602 10^{-19} C)
F	Faraday constant (96487 C mol^{-1})
j_i	Flux of ion i (mol m^{-2} s^{-1})
J_v	Permeation flux (m^3 m^{-2} s^{-1})
J_w	Permeation flux of pure water (m^3 m^{-2} s^{-1})
k_B	Boltzmann constant (96487 C.mol^{-1})
$K_{i,c}$	Ionic hindrance factor for convection (dimensionless)
$K_{i,d}$	Ionic hindrance factor for diffusion (dimensionless)
L_p	Hydraulic permeability (m^3 m^{-2})
R	Gas constant (8.314 J mol^{-1} K^{-1})
$r_{i,s}$	Stokes radius of ion i (m)
R_i	Observed rejection of ion i (dimensionless)
r_p	Average pore radius (m)
T	Temperature (K)
V	Solvent velocity in the pore (m.s^{-1})
x	Axial position within the pore (m)
X_d	Membrane effective charge density in the pore (eq m^{-3})
z_i	Valence of ion i (dimensionless)

- Greek letters

$\gamma_{i,p}$	activity coefficient of ion i in the pore (dimensionless)
$\gamma_{i,s}$	activity coefficient of ion i in the solution side of the interface (dimensionless)
ΔP	applied pressure (Pa)
ΔW_i	dielectric exclusion energy (J)
$\Delta\psi_D$	Donnan potential (V)
$\Delta\pi$	osmotic pressure difference (Pa)
ε_0	permittivity of free space (8.85419 10^{-12} F.m^{-1})
ε_b	bulk dielectric constant (dimensionless)
ε_p	pore dielectric constant (dimensionless)
μ	dynamic viscosity (Pa s)
ϕ_i	steric partition coefficient (dimensionless)
ψ	electrical potential within the pore (V)

References

[1] B. Van der Bruggen, E. Curcio, E. Drioli, Process intensification in the textile industry: the role of membrane technology, J. Environ. Manag., 73 (2004) 267-274.

[2] R.W. Baker, Membrane technology and applications., John Wiley & Sons, Chichester, 2004.

[3] D. Knorr, A. Froehling, H. Jaeger, K. Reineke, O. Schlueter, K. Schoessler, Emerging Technologies in Food Processing, Annu. Food. Sci. Technol., 2 (2011) 203-235.

[4] A.K. Pabby, S.S.H. Rizvi, A.M.S. Requena, Handbook of Membrane Separations: Chemical, Pharmaceutical, Food, and Biotechnological Applications, in, CRC Press, Boca Raton, 2015.

[5] B. Van der Bruggen, M. Mänttäri, M. Nyström, Drawbacks of applying nanofiltration and how to avoid them: A review, Sep. Purif. Technol., 63 (2008) 251-263.

[6] P. Mikulášek, J. Cuhorka, P. Doleček, Nanofiltration used for desalination in the liquid dye production, in: Nanofiltration: Applications, Advancements and Research, 2017, pp. 21-49.

[7] S.P. Dharupaneedi, S.K. Nataraj, M. Nadagouda, K.R. Reddy, S.S. Shukla, T.M. Aminabhavi, Membrane-based separation of potential emerging pollutants, Sep. Purif. Technol., 210 (2019) 850-866.

[8] P. Zhang, J.L. Gong, G.M. Zeng, C.H. Deng, H.C. Yang, H.Y. Liu, S.Y. Huan, Cross-linking to prepare composite graphene oxide-framework membranes with high-flux for dyes and heavy metal ions removal, Chem. Eng. J., 322 (2017) 657-666.

[9] X.Q. Cheng, Z.X. Wang, Y. Zhang, Y. Zhang, J. Ma, L. Shao, Bio-inspired loose nanofiltration membranes with optimized separation performance for antibiotics removals, J. Membr. Sci., 554 (2018) 385-394.

[10] G.S. Vieira, F.K.V. Moreira, R.L.S. Matsumoto, M. Michelon, F.M. Filho, M.D. Hubinger, Influence of nanofiltration membrane features on enrichment of jussara ethanolic extract (Euterpe edulis) in anthocyanins, J. Food Eng., 226 (2018) 31-41.

[11] D.P. Zagklis, C.A. Paraskeva, Isolation of organic compounds with high added values from agro-industrial solid wastes, J. Environ. Manag., 216 (2018) 183-191.

[12] R. Castro-Muñoz, V. Fíla, Membrane-based technologies as an emerging tool for separating high-added-value compounds from natural products, Trends Food Sci. Technol., 82 (2018) 8-20.

[13] G. Pearce, Introduction to membranes: Filtration for water and wastewater treatment, Filtr. Sep., 44 (2007) 24-27.

[14] R. Weber, H. Chmiel, V. Mavrov, Characteristics and application of new ceramic nanofiltration membranes, Desalination, 157 (2003) 113-125.

[15] J. Kim, B. Van der Bruggen, The use of nanoparticles in polymeric and ceramic membrane structures: Review of manufacturing procedures and performance improvement for water treatment, Environ. Pollut., 158 (2010) 2335-2349.

[16] F.C. Kramer, R. Shang, S.G.J. Heijman, S.M. Scherrenberg, J.B. Van Lier, L.C. Rietveld, Direct water reclamation from sewage using ceramic tight ultra- and nanofiltration, Sep. Purif. Technol., 147 (2015) 329-336.

[17] J. Xu, C.-Y. Chang, J. Hou, C. Gao, Comparison of approaches to minimize fouling of a UF ceramic membrane in filtration of seawater, Chem. Eng. J., 223 (2013) 722-728.

[18] R. Shang, A. Goulas, C.Y. Tang, X. de Frias Serra, L.C. Rietveld, S.G.J. Heijman, Atmospheric pressure atomic layer deposition for tight ceramic nanofiltration membranes: Synthesis and application in water purification, J. Membr. Sci., 528 (2017) 163-170.

[19] C. Adán, J. Marugán, S. Mesones, C. Casado, R. van Grieken, Bacterial inactivation and degradation of organic molecules by titanium dioxide supported on porous stainless steel photocatalytic membranes, Chem. Eng. J., 318 (2017) 29-38.

[20] M. Hatat-Fraile, R. Liang, M.J. Arlos, R.X. He, P. Peng, M.R. Servos, Y.N. Zhou, Concurrent photocatalytic and filtration processes using doped TiO2 coated quartz fiber membranes in a photocatalytic membrane reactor, Chem. Eng. J., 330 (2017) 531-540.

[21] Y. Liu, M. Peng, H. Jiang, W. Xing, Y. Wang, R. Chen, Fabrication of ceramic membrane supported palladium catalyst and its catalytic performance in liquid-phase hydrogenation reaction, Chem. Eng. J., 313 (2017) 1556-1566.

[22] S. Mozia, K. Szymański, B. Michalkiewicz, B. Tryba, M. Toyoda, A.W. Morawski, Effect of process parameters on fouling and stability of MF/UF TiO2 membranes in a photocatalytic membrane reactor, Sep. Purif. Technol., 142 (2015) 137-148.

[23] H. Choi, A.C. Sofranko, D.D. Dionysiou, Nanocrystalline TiO2 Photocatalytic Membranes with a Hierarchical Mesoporous Multilayer Structure: Synthesis, Characterization, and Multifunction, Adv. Funct. Mater., 16 (2006) 1067-1074.

[24] J. Hou, G. Dong, B. Xiao, C. Malassigne, V. Chen, Preparation of titania based biocatalytic nanoparticles and membranes for CO2 conversion, J. Mater. Chem. A, 3 (2015) 3332-3342.

[25] N. Rahimi, R.A. Pax, E.M. Gray, Review of functional titanium oxides. I: TiO2 and its modifications, Prog. Solid State Chem., 44 (2016) 86-105.

[26] R. Shang, A.R.D. Verliefde, J. Hu, Z. Zeng, J. Lu, A.J.B. Kemperman, H. Deng, K. Nijmeijer, S.G.J. Heijman, L.C. Rietveld, Tight ceramic UF membrane as RO pre-treatment: The role of electrostatic interactions on phosphate rejection, Water Res., 48 (2014) 498-507.

[27] S. Déon, P. Dutournié, L. Limousy, P. Bourseau, The two-dimensional pore and polarization transport model to describe mixtures separation by nanofiltration: Model validation, AIChE J., 57 (2011) 985-995.

[28] Z. Song, M. Fathizadeh, Y. Huang, K.H. Chu, Y. Yoon, L. Wang, W.L. Xu, M. Yu, TiO2 nanofiltration membranes prepared by molecular layer deposition for water purification, J. Membr. Sci., 510 (2016) 72-78.

[29] Y. Cai, X. Chen, Y. Wang, M. Qiu, Y. Fan, Fabrication of palladium–titania nanofiltration membranes via a colloidal sol–gel process, Microporous Mesoporous Mater., 201 (2015) 202-209.

[30] J. Luo, Y. Wan, Effects of pH and salt on nanofiltration—a critical review, J. Membr. Sci., 438 (2013) 18-28.

[31] V. Silva, Á. Martín, F. Martínez, J. Malfeito, P. Prádanos, L. Palacio, A. Hernández, Electrical characterization of NF membranes. A modified model with charge variation along the pores, Chem. Eng. Sci., 66 (2011) 2898-2911.

[32] S. Déon, P. Dutournié, L. Limousy, P. Bourseau, Transport of salt mixtures through nanofiltration

membranes: Numerical identification of electric and dielectric contributions, Sep. Purif. Technol., 69 (2009) 225-233.

[33] N. Pagès, M. Reig, O. Gibert, J.L. Cortina, Trace ions rejection tunning in NF by selecting solution composition: Ion permeances estimation, Chem. Eng. J., 308 (2017) 126-134.

[34] N.S. Kotrappanavar, A.A. Hussain, M.E.E. Abashar, I.S. Al-Mutaz, T.M. Aminabhavi, M.N. Nadagouda, Prediction of physical properties of nanofiltration membranes for neutral and charged solutes, Desalination, 280 (2011) 174-182.

[35] S. Bandini, D. Vezzani, Nanofiltration modeling: the role of dielectric exclusion in membrane characterization, Chem. Eng. Sci., 58 (2003) 3303-3326.

[36] A. Szymczyk, P. Fievet, Investigating transport properties of nanofiltration membranes by means of a steric, electric and dielectric exclusion model, J. Membr. Sci., 252 (2005) 77-88.

[37] M. Montalvillo, V. Silva, L. Palacio, J.I. Calvo, F.J. Carmona, A. Hernández, P. Prádanos, Charge and dielectric characterization of nanofiltration membranes by impedance spectroscopy, J. Membr. Sci., 454 (2014) 163-173.

[38] A. Efligenir, P. Fievet, S. Déon, R. Salut, Characterization of the isolated active layer of a NF membrane by electrochemical impedance spectroscopy, J. Membr. Sci., 477 (2015) 172-182.

[39] V. Freger, S. Bason, Characterization of ion transport in thin films using electrochemical impedance spectroscopy: I. Principles and theory, J. Membr. Sci., 302 (2007) 1-9.

[40] S. Déon, A. Escoda, P. Fievet, P. Dutournié, P. Bourseau, How to use a multi-ionic transport model to fully predict rejection of mineral salts by nanofiltration membranes, Chem. Eng. J., 189-190 (2012) 24-31.

[41] P. Dutournié, L. Limousy, J. Anquetil, S. Déon, Modification of the selectivity properties of tubular ceramic membranes after alkaline treatment, Membranes, 7 (2017).

[42] J. Bikaï, L. Limousy, P. Dutournié, L. Josien, W. Blel, Stabilisation of the water permeability of mineral ultrafiltration membranes: An empirical modelling of surface and pore hydration, C. R. Chim., 18 (2015) 56-62.

[43] S. Déon, B. Lam, P. Fievet, Application of a new dynamic transport model to predict the evolution of performances throughout the nanofiltration of single salt solutions in concentration and diafiltration modes, Water Res., 136 (2018) 22-33.

[44] T.R. Noordman, J.A. Wesselingh, Transport of large molecules through membranes wiyh narrow pores. The Maxwell-Stefan description combined with hydrodynamic theory, J. Membr. Sci., 210 (2002) 227-243.

[45] T. Tsuru, S. Izumi, T. Yoshioka, M. Asaeda, Temperature effect on transport performance by inorganic nanofiltration membranes, AIChE J., 46 (2000) 565-574.

[46] W.R. Bowen, J.S. Welfoot, Modelling the performance of membrane nanofiltration-critical assessment and model development, Chem. Eng. Sci., 57 (2002) 1121-1137.

[47] J. Schaep, C. Vandecasteele, A.W. Mohammad, W.R. Bowen, Modelling the retention of ionic components for different nanofiltration membranes, Sep. Purif. Technol., 22-23 (2001) 169.

[48] A.A. Hussain, S.K. Nataraj, M.E.E. Abashar, I.S. Al-Mutaz, T.M. Aminabhavi, Prediction of physical properties of nanofiltration membranes using experiment and theoretical models, J. Membr.

Sci., 310 (2008) 321-336.

[49] S. Déon, P. Dutournié, P. Fievet, L. Limousy, P. Bourseau, Concentration polarization phenomenon during the nanofiltration of multi-ionic solutions: Influence of the filtrated solution and operating conditions, Water Res., 47 (2013) 2260-2272.

[50] W.R. Bowen, J.S. Welfoot, P.M. Williams, Linearized transport model for nanofiltration: Development and assessment, AIChE J., 48 (2002) 760-773.

[51] J.D. Ferry, Statistical evaluation of sieve constants in ultrafiltration, The Journal of General Physiology, 20 (1935) 95-104.

[52] P. Dutournié, L. Limousy, W. Blel, S. Déon, P. Fievet, Understanding of ion transport in a na-mordenite membrane: Use of numerical modeling to estimate surface-solute interactions in the pore, Ind. Eng. Chem. Res., 53 (2014) 8221-8227.

[53] C. Combe, C. Guizard, P. Aimar, V. Sanchez, Experimental determination of four characteristics used to predict the retention of a ceramic nanofiltration membrane, J. Membr. Sci., 129 (1997) 147-160.

[54] W.R. Bowen, A.W. Mohammad, N. Hilal, Characterisation of nanofiltration membranes for predictive purposes - use of salts, uncharged solutes and atomic force microscopy, J. Membr. Sci., 126 (1997) 91-105.

[55] A. Escoda, S. Déon, P. Fievet, Assessment of dielectric contribution in the modeling of multi-ionic transport through nanofiltration membranes, J. Membr. Sci., 378 (2011) 214-223.

[56] P. Árki, C. Hecker, G. Tomandl, Y. Joseph, Streaming potential properties of ceramic nanofiltration membranes – Importance of surface charge on the ion rejection, Sep. Purif. Technol., 212 (2019) 660-669.

Graphical Abstract